

Estimation of sound power of baffled planar sources using radiation matrices

Mingsian R. Bai^{a)} and Mingchun Tsao

Department of Mechanical Engineering, National Chiao-Tung University, Hsin-Chu 30010, Taiwan, Republic of China

(Received 2 October 2001; revised 24 May 2001; accepted 11 June 2002)

A technique is presented in this paper for the analysis of acoustic radiation of baffled planar sources. This method is based on the concept of the radiation matrix which is a representation of the sound field radiated by complex sources. Both sound power and far-field pressure can be estimated using this method. Numerical simulation and experimental investigation were carried out to verify the proposed method. In comparison with the conventional pressure-based method ISO 3745, the proposed technique produced more accurate estimation of sound power. With comparable number of measuring positions as the conventional methods, the proposed approach does not require special measuring environments. Computation complexity can be significantly reduced if only dominant radiation modes in the low-frequency range are retained. Estimation of far-field pressure can also be obtained using the proposed method. © 2002 Acoustical Society of America.

[DOI: 10.1121/1.1499133]

PACS numbers: 43.20.Rz, 43.40.Rj [MO]

I. INTRODUCTION

Sound power is an important index in acoustic radiation analysis because it is a single global quantity which can be used to characterize the strength of the sound generated by a source. Estimation of sound power is also a common practice of identifying dominant sources prior to a noise control project. Many standard methods are available for sound power estimation.¹ Some of them are based on pressure measurement; the others are based on intensity measurement. Some of them require free-field environment; the others require diffuse field environment.

In this paper, a technique different from the earlier methods is presented. This method is based on the concept of *radiation matrix* which is a representation of the sound field radiated by complex sources. More precisely, radiation modes are “vibration” patterns on the surface of a structure that radiate orthogonal sound fields into the space.^{2–6} In the past, the ideas of radiation matrix and radiation modes have mainly been employed in the application of *Active Structural Acoustical Control (ASAC)*^{2,3} to control low-frequency noise radiated by vibrating surfaces. In this paper, however, this idea of radiation modes is exploited to deal with a different problem—estimation of sound power and far-field pressure radiated from complex baffled planar sources. In addition, an experimental procedure using the radiation mode concept is established in this work, in an attempt to achieve improved estimation over conventional approaches.

Complexity of the calculation can be further reduced if only the dominant radiation modes are retained in the computation. A crucial step of this procedure is the replacement of the frequency-dependent radiation modes by frequency-independent ones.^{7,8} In ASAC, the “radiation filter” consists of a constant modal filtering matrix, cascaded with frequency-dependent radiation efficiency filters.

As demonstrated by Berkhoff,⁹ the input to the radiation filter can be based on either surface velocity data or near-field pressure data. This paper adopts primarily the former approach because, from our experience, it provides more reliable results than the latter approach. The pressure-based methods are thus omitted for brevity. With comparable number of measuring positions as the conventional methods, the proposed techniques do not require special measuring environment, e.g., a reverberant room or an anechoic room because only surface velocity is required as the input data.

This paper mainly focuses on baffled planar sources. Two kinds of sound sources, a baffled rigid piston and a baffled point-driven flexible plate, are chosen as the test objects in the simulation. The surface vibration of the plate is calculated by using ANSYS.¹⁰ Sound power and far-field pressure are calculated. The proposed techniques are verified by numerical simulation as well as experiments. A baffled vibrating plate is chosen as the test source. The proposed methods are also compared with the ISO 3745 (Ref. 11) which is a widely accepted standard for sound power estimation.

II. RADIATION MATRIX-BASED TECHNIQUES

A. Velocity-based full radiation mode method (VFRM)

For a sound source with surface A , the radiated sound power W can be calculated by

$$W = \frac{S}{2} \text{Re}\{\mathbf{v}^H \mathbf{p}\}, \quad (1)$$

where S is the area of each element, \mathbf{p} and \mathbf{v} are pressure vector and velocity vector, respectively, on the surface, and the superscript “ H ” denotes the Hermitian transpose operator.

On the surface of the source, the pressure vector \mathbf{p} can be related to the velocity vector \mathbf{v} by the following equation:

^{a)}Electronic mail: msbai@cc.nctu.edu.tw

$$\mathbf{p} = \mathbf{Z}\mathbf{v}, \quad (2)$$

where \mathbf{Z} is the radiation impedance matrix that in general can be obtained using numerical methods such as boundary element methods.¹² There exist a number of different definitions of impedance in acoustics. The matrix \mathbf{Z} is termed radiation matrix simply because it relates the pressure and velocity distributions on a acoustically radiating surface of a source. The dimension of the matrix \mathbf{Z} , however, is the same as specific acoustic impedance, i.e., pressure/velocity. For a baffled planar source, however, the matrix \mathbf{Z} can simply be calculated by using the following formula:⁹

$$\mathbf{Z} = \rho_0 c \begin{bmatrix} d & -\frac{jkS}{2\pi} \frac{e^{ikr_{12}}}{r_{12}} & \dots & -\frac{jkS}{2\pi} \frac{e^{ikr_{1N}}}{r_{1N}} \\ -\frac{jkS}{2\pi} \frac{e^{ikr_{21}}}{r_{21}} & d & \dots & \vdots \\ \vdots & \vdots & \dots & \vdots \\ -\frac{jkS}{2\pi} \frac{e^{ikr_{N1}}}{r_{N1}} & \dots & \dots & d \end{bmatrix}, \quad (3)$$

where

$$d = \frac{1}{2} \left(k \sqrt{\frac{S}{\pi}} \right)^2 - j \frac{8}{3\pi} \left(k \sqrt{\frac{S}{\pi}} \right), \quad (4)$$

ρ_0 is the air density, c is the sound speed, $k = \omega/c$ is the wave number, and $r_{mn} = r_{nm}$ is the distance from the element m to the element n , $1 \leq m, n \leq N$. Equation (4) is based on a numerical approximation of the Rayleigh integral in which the field point approaches the source surface. The off-diagonal elements are contributions due to point sources of the elemental radiators, with given volume velocity which lead to pressure on the other elements on the surface. For the diagonal terms, the field point and the source point may coincide, which results in a singular problem. The difficulty can be circumvented if the integration is not over a square area but over a circular area. The approach leads to an approximation of the diagonal terms. Note that the expressions of the diagonal terms are somewhat different from that in Ref. 9.

Equations (2) and (3) lead to

$$\mathbf{W} = \mathbf{v}^H \mathbf{R} \mathbf{v}, \quad (5)$$

where the radiation resistance matrix $\mathbf{R} = S \operatorname{Re}\{\mathbf{Z}\}/2$ can be calculated by

$$\mathbf{R} = \frac{\omega^2 \rho_0 S^2}{4\pi c} \begin{bmatrix} 1 & \frac{\sin(kr_{12})}{kr_{12}} & \dots & \frac{\sin(kr_{1N})}{kr_{1N}} \\ \frac{\sin(kr_{21})}{kr_{21}} & 1 & \dots & \vdots \\ \vdots & \vdots & \dots & \vdots \\ \frac{\sin(kr_{N1})}{kr_{N1}} & \dots & \dots & 1 \end{bmatrix}. \quad (6)$$

Complexity of the computation can be further reduced if only the dominant modes are retained in the computation. This is accomplished by exploiting the fact that \mathbf{R} is a real-

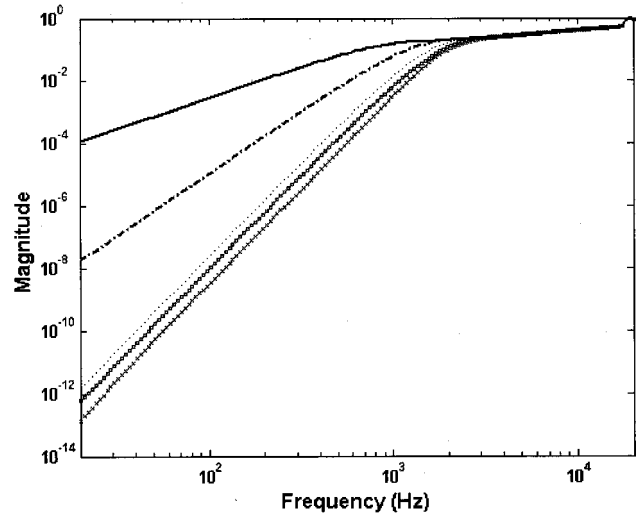


FIG. 1. The radiation efficiencies of the first six radiation modes of the baffled piston (—, first singular value; ---, second singular value; - · -, third singular value; · · ·, fourth singular value, □, fifth singular value; +, sixth singular value).

symmetric and positive-definite matrix and the following eigenvalue decomposition (EVD) is always possible¹³

$$\mathbf{R} = \mathbf{Q}^T \mathbf{\Lambda} \mathbf{Q}, \quad (7)$$

where $\mathbf{\Lambda} = \operatorname{diag}(\lambda_1, \lambda_2, \dots, \lambda_L)$ are eigenvalues that have the physical meaning as the radiation efficiencies, the radiation modal filter $\mathbf{Q} = [\mathbf{q}_1, \mathbf{q}_2, \dots, \mathbf{q}_L]$ is a group of orthogonal surface vibration patterns associated with the radiation modes. These radiation modes are associated with surface velocity distributions that produce orthogonal sound pressure modes which are generally different from the actual acoustical modes that satisfy boundary conditions. Although these radiation modes are always orthogonal in the mathematical sense, they are generally different from the structural vibration modes. In practice, only a limited number, say L , of radiation modes that are efficient in low frequencies. The computation can be simplified by considering only these dominant modes. From Eqs. (5) and (7),

$$\mathbf{W} = \mathbf{y}^H \mathbf{\Lambda} \mathbf{y} = \sum_{i=1}^L \lambda_i |y_i|^2, \quad (8)$$

where vector $\mathbf{y} = \mathbf{Q}\mathbf{v}$. Each diagonal element represents the radiation efficiency corresponding to each radiation mode. Note that the radiation efficiency can be related to radiation resistance (real part of radiation impedance) normalized with $\rho_0 c$. Modes with large λ_i values are the modes capable of propagating efficiently into far field, whereas modes with small λ_i values are the *evanescent modes* existing only in near field. Figure 1 shows the radiation efficiencies of the first six radiation modes for a baffled rigid piston with 0.1 m radius. Note that, in the low-frequency range ($ka < 1$, a is the radius), only two to six modes are dominant. At the extreme ($ka \ll 1$), the first mode (the volume velocity mode) is the only efficient mode. At the other extreme ($ka \gg 1$), all radiation modes contribute equally to the radiation with unity efficiency. This motivates the use of low-order radiation modes

to represent the sound field for low frequency range such that the computation can be simplified.

However, the radiation modal matrix is frequency dependent, which requires the computation procedure to be repeated for each frequency. A remedy to this difficulty lies in the fact that the radiation modes are slowly varying with respect to frequency and the low-frequency modes are “nested” by the high-frequency modes.² Figures 2(a) and (b) show the radiation modes of a baffled piston with a radius 0.1 m for $kl=0.1$ and $kl=2$. Now, suppose sound power is to be estimated by measuring the surface velocity at M positions on a source. The size of matrix \mathbf{R} will be $M \times M$, which calls for the need of M^2 filters. Instead of using frequency-dependent matrices, the computation load can be reduced by using the radiation modal matrix, \mathbf{Q}_{\max} , at the highest frequency of interest. Note that \mathbf{Q}_{\max} is a constant matrix with the dimension $M \times L$, where $L \ll M$ represents the number of dominant radiation modes. On the other hand, the radiation efficiency of the i th mode can be approximated as

$$\lambda_i(j\omega) = \mathbf{q}_{i,\max} \mathbf{R}(j\omega) \mathbf{q}_{i,\max}^T, \quad (9)$$

where $\mathbf{q}_{i,\max}$ is the i th column of \mathbf{Q}_{\max} , λ_i is still a function of frequency and generally exhibits a high-pass behavior. Hence, sound power can be estimated by the velocity-based dominant radiation mode method (VDRM):

$$W = \mathbf{v}^H \tilde{\mathbf{R}} \mathbf{v}, \quad (10)$$

where the matrix $\tilde{\mathbf{R}}$ is approximated as

$$\tilde{\mathbf{R}} = \mathbf{Q}_{\max}^T \tilde{\Lambda} \mathbf{Q}_{\max}, \quad (11)$$

where $\tilde{\Lambda} = \text{diag}[\lambda_1(j\omega), \lambda_2(j\omega), \dots, \lambda_L(j\omega)]$. In this setting, only a constant matrix \mathbf{Q}_{\max} and L filters are needed in the computation.

B. Modified velocity-based dominant radiation modes method (MVDRM)

The VDRM is based on the idea of dominant radiation mode which is only true in low frequencies. In high frequencies, direct use of VDRM will give rise to errors because all modes contribute equally to sound radiation. To correct the problem for high frequencies, we use another approach to estimate the sound power. For high frequencies, e.g., $ka > 4$, the waves radiated from a planar source behave like plane waves and Eq. (5) should be modified into

$$W = \rho_0 c A \frac{\sum_{i=1}^N \nu_{\text{rms},i}^2}{N}, \quad (12)$$

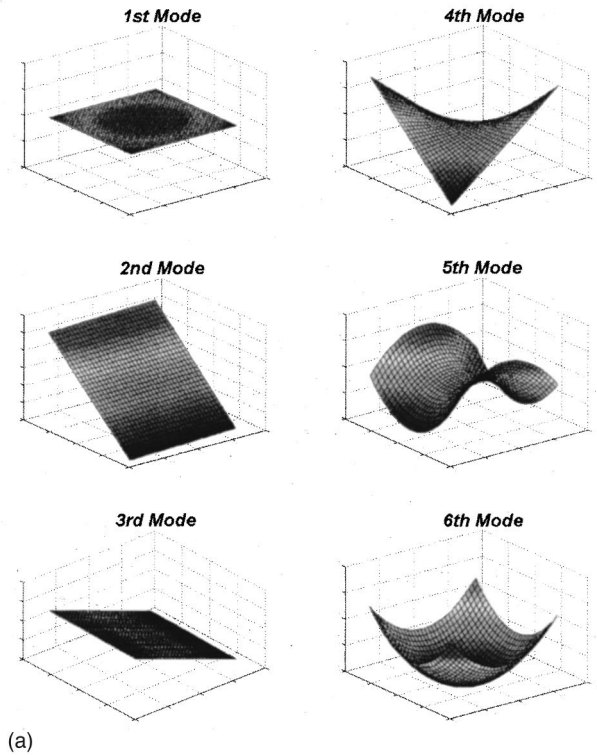
where ρ_0 is the air density, A is the total surface area of the source, c is the sound speed, ν_{rms} is the root-mean-square normal velocity, and N is the number of measurements.

C. Far-field pressure

Apart from sound power, far-field sound pressure can also be calculated by using the idea of radiation modes. The Rayleigh integral can be discretized into a matrix equation

$$\mathbf{p} = \mathbf{E} \mathbf{v}, \quad (13)$$

$ka=0.1$



$ka=2$

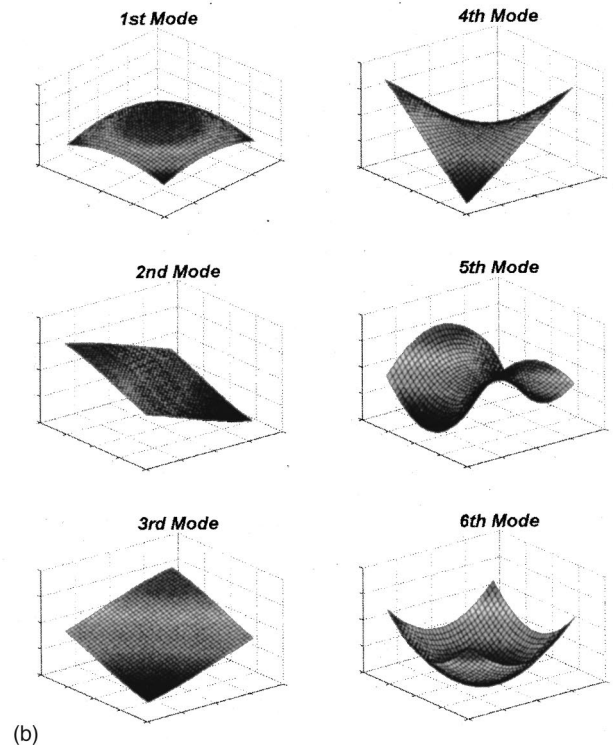


FIG. 2. The first six radiation modes. (a) $ka=0.1$; (b) $ka=2$.

where \mathbf{p} is the vector of far-field pressure, \mathbf{E} is the propagation matrix, and \mathbf{v} is the vector of surface velocity.

For a baffled planar radiator, this propagation matrix \mathbf{E} can be approximated as⁹

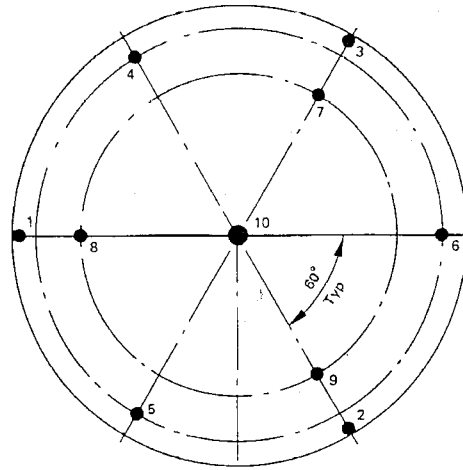
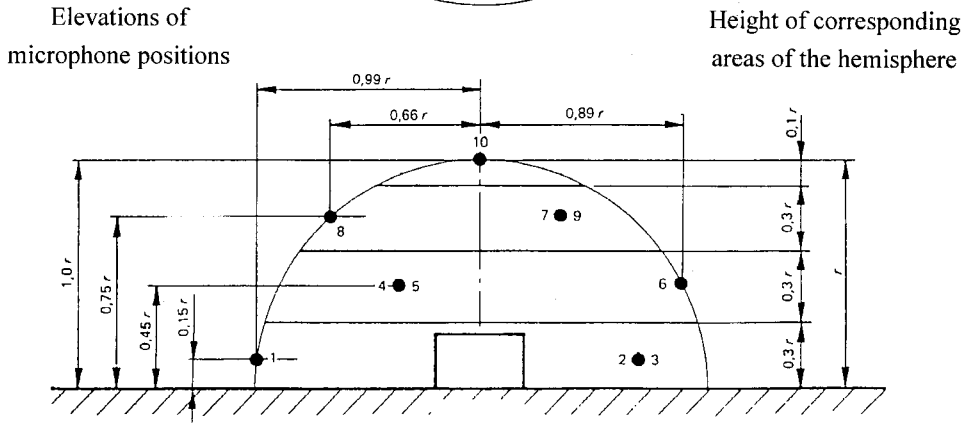


FIG. 3. Microphone positions on a hemispherical surface surrounding a source whose sound power level is to be measured according to ISO 3745 (cited from Ref. 11).



$$\mathbf{E} = j \frac{\rho_0 c k S}{2\pi} \begin{bmatrix} \frac{e^{-jkr_{11}}}{r_{11}} & \frac{e^{-jkr_{12}}}{r_{12}} & \dots & \frac{e^{-jkr_{1N}}}{r_{1N}} \\ \frac{e^{-jkr_{21}}}{r_{21}} & \frac{e^{-jkr_{22}}}{r_{22}} & \dots & \frac{e^{-jkr_{2N}}}{r_{2N}} \\ \vdots & \vdots & \dots & \vdots \\ \frac{e^{-jkr_{M1}}}{r_{M1}} & \frac{e^{-jkr_{M2}}}{r_{M2}} & \dots & \frac{e^{-jkr_{MN}}}{r_{MN}} \end{bmatrix}, \quad (14)$$

where r_{MN} is the distance from the elemental radiator N to the field point M .

Similar to power estimation, SVD¹³ can be applied to the propagation matrix \mathbf{E} , i.e.,

$$\mathbf{E} = \mathbf{U} \mathbf{\Lambda} \mathbf{V}^H, \quad (15)$$

where the diagonal matrix $\mathbf{\Lambda}$ has singular values as its diagonal, \mathbf{U} and \mathbf{V} are unitary matrices. In low-frequency range, only several dominant modes are needed to represent the propagation process.¹⁴ That is,

$$\tilde{\mathbf{E}} = \tilde{\mathbf{U}} \tilde{\mathbf{\Lambda}} \tilde{\mathbf{V}}^H. \quad (16)$$

Thus, the far-field sound pressure \mathbf{p} and \mathbf{v} can be approximated as

$$\tilde{\mathbf{p}} = \tilde{\mathbf{E}} \mathbf{v}. \quad (17)$$

III. NUMERICAL AND EXPERIMENTAL INVESTIGATIONS

In this section, numerical simulation and experimental investigation were carried out to verify the proposed method.

A. Sound power estimation

1. Case 1—baffled rigid piston

In this example, we use a baffled rigid piston as a sound source to verify the proposed methods, VFRM, VDRM, and MVDRM. The piston source is chosen because its power can be calculated analytically.¹⁵ The radius of the piston is 0.1 m which is excited with surface velocity $1 \cdot e^{j\omega t}$ cm/s.

To justify the proposed techniques, a widely used ISO standard 3745 for sound power estimation in free-field environment is also employed in the comparison. The ISO procedure requires the mean value calculated from the pressure measurements at 10 positions on hemispherical surface surrounding the source of interest, as shown Fig. 3. The method is essentially based on the assumption of a point source, which is approximately true in the far field. Figure 4 compares the estimations of sound power obtained using the theoretical model and the ISO standard, respectively. Deviations from the theoretical value are found in high-frequency range (>1 kHz), using the ISO method. The total sound power within the band 20–16 kHz are found to be 88.1 dB and 96.3 dB for the theoretical value and ISO 3745, respectively. The

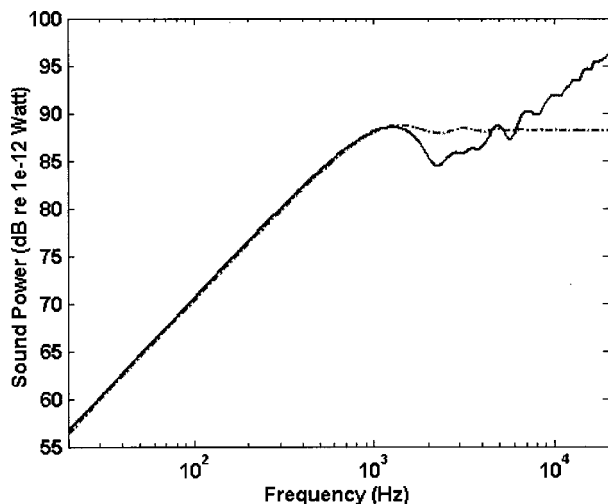


FIG. 4. The comparison of sound power radiated by the baffled piston between the theoretical calculation and ISO 3745 (---, theoretical value; —, ISO 3745).

errors in power estimation using ISO 3745 can be explained as follows. ISO 3745 is an essentially pressure-based method under the free-field condition. The measurement should be conducted in a sufficiently far field so that it can be approximated by a point source field. However, even under the free-field condition, there are possibly three types of errors in the measurement: (1) the near field error, (2) a limited number of measuring points, and (3) the error in sound pressure measurement. A detailed investigation on these issues can be found in Ref. 16.

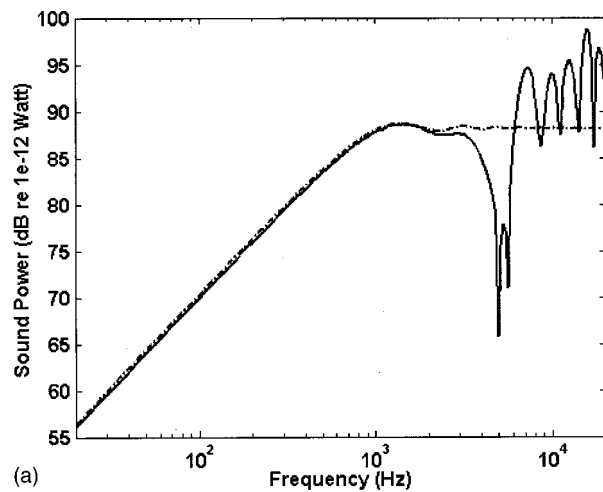
The proposed power estimation method requires velocity measurements at the grid points on the source surface. First, the sound power radiated by the piston is estimated by VFRM. A 4×4 rectangular mesh (16 elements) is used. Figure 5(a) compares the estimations of sound power obtained using the theoretical model and VFRM, respectively. The approximation appears close to the theoretical value in the low-frequency range ($ka < 4$, $f < 1000$ Hz), while some deviations are found in the high-frequency range.

Next, VDRM is applied to estimate the sound power for the same frequency range ($ka < 4$, $f < 1000$ Hz). Similar estimation of the radiated sound power is obtained by using only the first six radiation modes, as shown in Fig. 5(b).

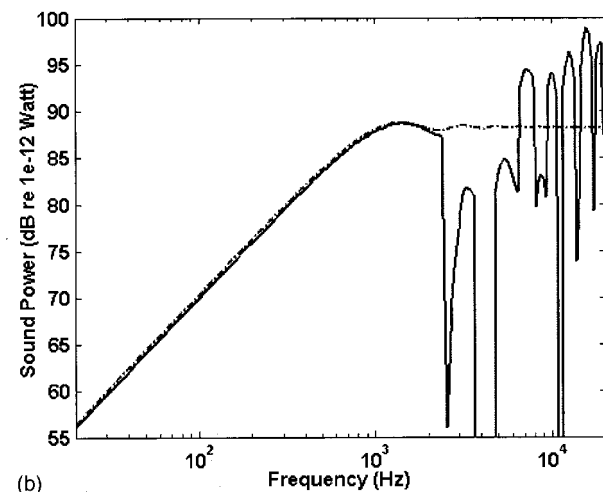
The foregoing results indicate that VFRM and VDRM are able to give accurate estimation only in the low-frequency range. For the high-frequency range, the modified method MVDRM should be used to produce estimations with less error. Figure 5(c) compares the estimations of sound power obtained using the theoretical model and MVDRM, respectively. The total sound power within the band 20–16 kHz are found to be 88.1 dB, 86.5 dB, 86.1 dB, and 87.9 dB for the theoretical value, VFRM, VDRM, and MVDRM, respectively. From the result, MVDRM is found to produce the best estimation of sound power in both the low and high frequencies.

2. Case 2—vibrating plate

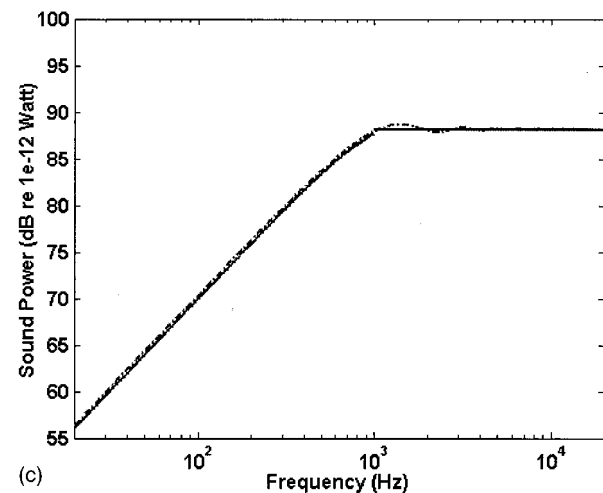
The rigid piston used for the last simulation has uniform surface velocity distribution. A more complex sound source,



(a)



(b)



(c)

FIG. 5. The comparison of sound power radiated by the baffled piston between the theoretical calculation and the proposed methods. (a) The theoretical calculation versus VFRM (4×4 mesh) (---, theoretical value; —, VFRM); (b) the theoretical calculation versus VDRM by using the first six modes (4×4 mesh) (---, theoretical value; —, VDRM); (c) the theoretical calculation versus MVDRM (4×4 mesh) (---, theoretical value; —, MVDRM).

a vibrating flexible plate shall be used as the test sound source in this case. The parameters of the plate are area $= 0.2 \times 0.15$ m², density $\rho = 246$ kg/m³, Young's modulus $E = 2.28 \times 10^9$ N/m², Poisson ratio $\nu = 0.33$, and thickness h

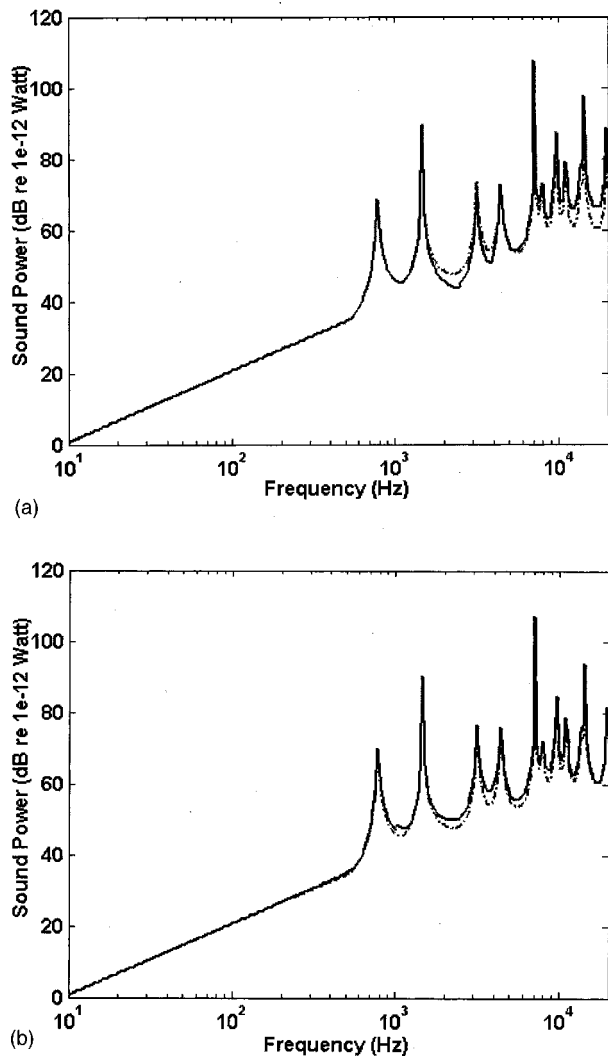


FIG. 6. The sound power radiated by the vibrating plate. (a) Theoretical calculation versus ISO 3745 (---, theoretical value; —, ISO 3745); (b) the theoretical calculation versus MVDRM by using the first six modes (3×3 mesh) (---, theoretical value; —, MVDRM).

$= 1$ cm. The plate is excited at the center by a time-harmonic concentrated force, $0.5e^{j\omega t}N$. Four boundaries of the plate are assumed free. Finite element software, ANSYS, is employed to calculate the normal velocity distribution on the surface. Sound power is then estimated by using a 32×32 \mathbf{R} matrix. Unlike rigid pistons, there is no analytical solution of sound power for plates, and thus we are content with the use of the fine mesh (32×32) as the “theoretical” solution.

Figure 6(a) compares the estimations of sound power obtained using the theoretical model and ISO 3745, respectively. In contrast to the piston, peaks due to resonance of the plate can be clearly seen in the spectrum. Deviations from the theoretical value are found in the high-frequency range (> 1 kHz), using the ISO method.

Next, the modified method, MVDRM, is utilized to estimate the sound power radiated by the plate. Figure 6(b) compares the estimations of sound power obtained using the theoretical model and MVDRM, respectively. The total sound power within the band 20–16 kHz are found to be 77.6 dB, 76.2 dB, and 77.1 dB for the theoretical value, ISO

3745, and MVDRM, respectively. It is then concluded from the numerical comparison that, with comparable number of measurements (9 vs 10), MVDRM produces more accurate estimation of sound power than the ISO method.

B. The far-field radiation

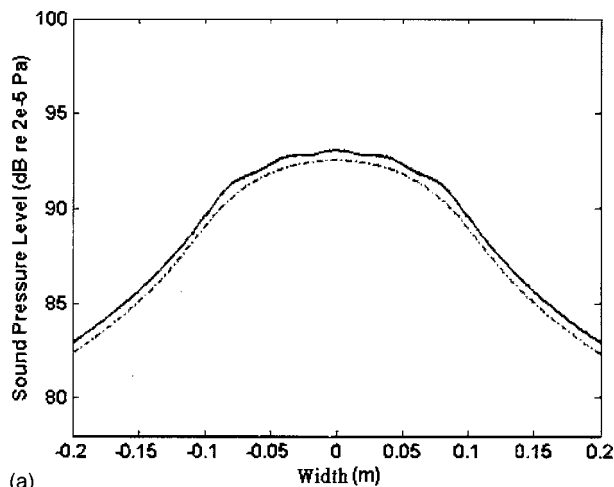
In this section, calculation of far-field sound pressure using the proposed techniques will be examined, particularly in terms of propagation distance and the number of modes used in SVD of the matrix \mathbf{E} .

The parameters of the baffled piston used in the simulations are identical to those mentioned earlier. The “theoretical” values of the piston can be calculated by using a very fine mesh, e.g., 32×32 . To examine the effect of propagation distance, a dimensionless parameter, the Fresnel number,¹⁵ is defined as follows:

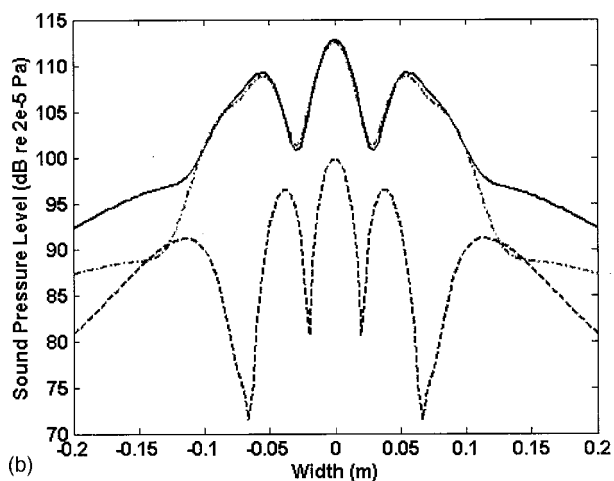
$$FN = \frac{r\lambda}{a^2}, \quad (18)$$

where r is the axial distance from the piston surface to the field point, λ is the wavelength, and a is the radius of piston. Figure 7(a) compares the far-field sound pressure obtained using the theoretical model, \mathbf{E} matrix based on 5×5 mesh with full modes, and \mathbf{E} matrix based on 5×5 mesh with the first six modes, respectively, for $ka = 0.5$ and $FN = 2$. The result of approach using the first six modes coincides with that using full modes, and so we found only a single dashed curve in the figure. Figure 7(b) compares the far-field sound pressure obtained using the theoretical model, \mathbf{E} matrix based on 11×11 mesh with full modes, and \mathbf{E} matrix based on 11×11 mesh with the first six modes, respectively, for $ka = 30$ and $FN = 2$. As expected, to calculate the far-field sound pressure for a source with a large ka value requires a matrix \mathbf{E} with higher dimension. Conversely, it takes only a few dominant modes to reconstruct far-field sound pressure for sources with a small ka value.

Like power estimation, we also apply the proposed technique to calculate the far-field sound pressure radiated by the vibrating plate. Finite element software, ANSYS, is employed to calculate the normal velocity distribution on the surface. Sound power is then estimated by numerically calculating the Rayleigh integral. Since there is no analytical solution of sound pressure for plates, we are content with the use of the fine mesh (32×32) as the “theoretical” solution. Figure 8(a) compares the far-field sound pressure obtained using the theoretical model, \mathbf{E} matrix based on a 5×5 mesh with full modes, and \mathbf{E} matrix based on a 5×5 mesh with the first six modes, respectively, for $ka = 1.5$ and $FN = 5$, where a is the shorter width of the plate edges. Figure 8(b) compares the far-field sound pressure obtained using the theoretical model, \mathbf{E} matrix based on a 11×11 mesh with full modes, and \mathbf{E} matrix based on a 11×11 mesh with the first six modes, respectively, for $ka = 20$ and $FN = 0.1$. As in the case of piston, to calculate the far-field sound pressure for a source with a large ka value requires a matrix \mathbf{E} with higher dimension. Conversely, it takes only a few dominant modes to reconstruct far-field sound pressure for sources with a small ka value.



(a)



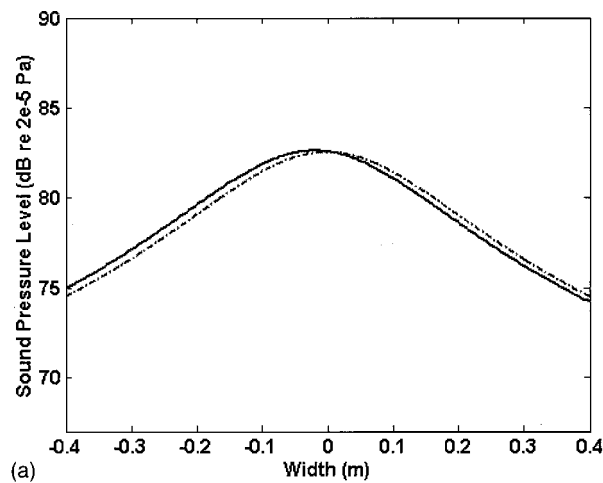
(b)

FIG. 7. Comparison of the far-field sound pressure radiated by the baffled piston, obtained using the theoretical model, E matrix with full modes, and E matrix with the first six modes. (a) 5×5 mesh, $ka=0.5$ and $FN=2$; (b) 11×11 mesh, $ka=30$ and $FN=0.2$ (---, theoretical value; —, E with full modes; - - -, E with six modes).

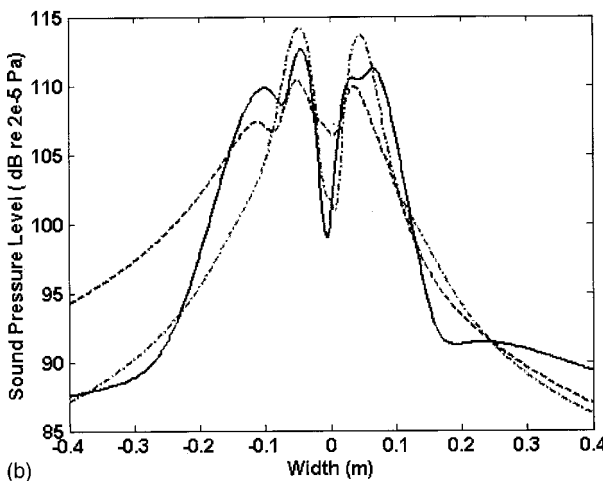
C. Experimental investigation of the vibrating plate

In addition to the forgoing numerical simulations, experiments were carried out for a vibrating plate in order to further verify the proposed techniques. The experimental arrangement is shown in Fig. 9. The experimental rig consists of primarily a PU-foam panel embedded in a wooden baffle. The dimensions of the panel are $0.113 \text{ m} \times 0.2 \text{ m} \times 0.002 \text{ m}$. The material properties of the panel are density $\rho = 246 \text{ kg/m}^3$, Young's modulus $E = 2.28 \times 10^9 \text{ N/m}^2$, Poisson ratio $\nu = 0.33$. The panel is excited at the center by a small electromagnetic shaker. A fiber optic displacement sensor (PHILTEC, D125) is used to measure the surface velocities at the nine grid points on the vibrating panel.

In this experiment, the MVDRM method and the ISO 3745 are compared to the numerical model. Sound power calculated by using the aforementioned ANSYS and Rayleigh integral, with exciter response taken into account, serves as the "theoretical" value for comparison. The ISO method is conducted in an anechoic room. With comparable number of measuring positions as the conventional methods, the proposed method is conducted in an ordinary room be-



(a)



(b)

FIG. 8. Comparison of the far-field sound pressure radiated by the vibrating plate, obtained using the theoretical model, E matrix with full modes, and E matrix with the first six modes. (a) 5×5 mesh, $ka=1.5$ and $FN=5$; (b) 11×11 mesh, $ka=20$ and $FN=0.1$ (---, theoretical value; —, E with full modes, - - -, E with six modes).

cause only surface velocity is required as the input data. A requirement of the proposed method is that the measurement must be conducted for planar sources baffled in a rigid infinite plane. Figure 10 shows the results obtained using these three approaches. The total sound power within the band 20–16 kHz are found to be 72.2 dB, 65.3 dB, and 69.4 dB

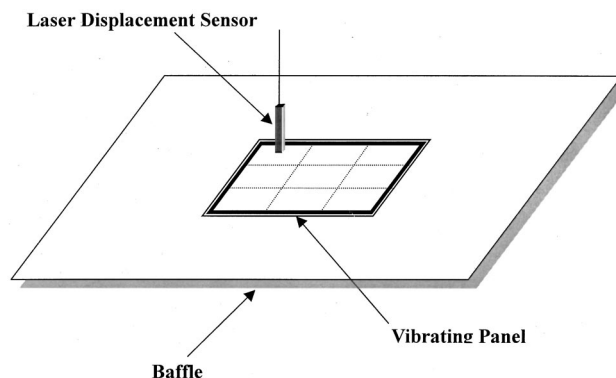


FIG. 9. The experimental arrangement of a baffled vibrating panel for sound power estimation.

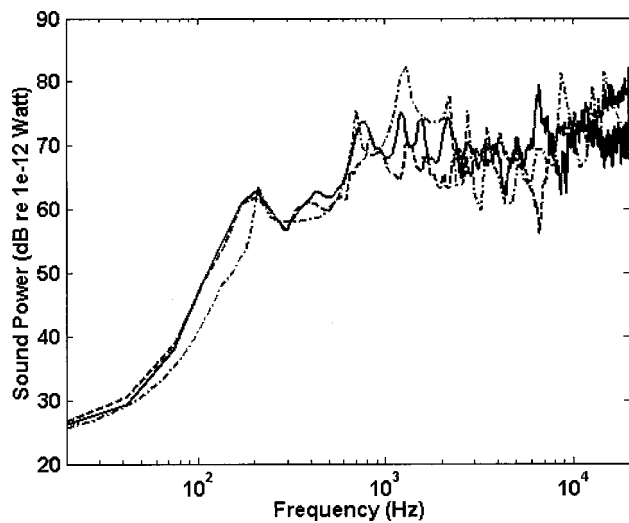


FIG. 10. Experimental results of sound power estimation for the baffled vibrating panel (---, theoretical value; - · -, ISO 3745; —, MVFRM).

for the theoretical value, ISO 3745, and MVDRM, respectively. Similar to the observation in numerical simulation, the experimental investigation indicates the proposed method provides a better estimation of sound power than the ISO standard.

IV. CONCLUSIONS

A technique based on radiation matrix is presented in this paper for the analysis of acoustic radiation of baffled planar sources. Numerical simulation and experimental investigation were carried out to verify the methods. From numerical and experimental results, the proposed method proves to be useful in estimating sound power and far-field pressure radiated by a complex source. In comparison with the conventional method, ISO 3745, the proposed techniques produced closer estimation of sound power. With comparable number of measuring positions as the conventional method, the proposed approach does not require special measuring environments. In addition, to calculate the far-field sound pressure for a source with a large ka value requires a matrix E with higher dimension. Conversely, it takes only a few dominant modes to reconstruct far-field sound pressure for sources with a small ka value.

As a limitation of the proposed techniques, the sound sources are restricted to planar sources baffled in a rigid infinite plane. By more sophisticated numerical schemes, e.g., the boundary element methods, the same rationale can be readily extended to deal with more practical problems such as radiation from three-dimensional sources. This aspect will be explored in future research.

ACKNOWLEDGMENTS

This work was supported by the National Science Council in Taiwan, Republic of China, under the Project No. NSC 89-2212-E009-057.

- ¹J. R. Hasall and K. Zaveri, *Acoustic Noise Measurements* (Bruel & Kjaer, Denmark, 1988).
- ²R. L. Clark, W. R. Saunders, and G. P. Gibbs, *Adaptive Structures* (Wiley, New York, 1998).
- ³S. J. Elliott and M. E. Johnson, "Radiation modes and the active control of sound power," *J. Acoust. Soc. Am.* **94**, 2194–2204 (1993).
- ⁴G. V. Borgiotti and K. E. Jones, "The determination of the acoustic far field of a radiating body in an acoustic fluid from boundary measurements," *J. Acoust. Soc. Am.* **93**, 2788–2797 (1993).
- ⁵M. N. Currey and K. A. Cunefare, "The radiation modes of baffled finite plates," *J. Acoust. Soc. Am.* **98**, 1570–1580 (1995).
- ⁶B. S. Cazzolato, "Sensing systems for active control of sound transmission into cavities," Ph.D. thesis, University of Adelaide, 1999.
- ⁷G. V. Borgiotti and K. E. Jones, "Frequency independence property of radiation spatial filters," *J. Acoust. Soc. Am.* **96**, 3516–3524 (1994).
- ⁸W. T. Baumann, W. R. Saunders, and H. H. Robertshaw, "Active suppression of acoustic radiation from impulsively excited structures," *J. Acoust. Soc. Am.* **90**, 3202–3208 (1991).
- ⁹A. P. Berkhoff, "Sensor scheme design for active structural acoustic control," *J. Acoust. Soc. Am.* **108**, 1037–1045 (2000).
- ¹⁰P. Kohnke, Theory Reference, ANSYS, 1994.
- ¹¹ISO 3745, *Acoustics—Determination of sound power levels of noise sources—Precision methods for anechoic and semi-anechoic rooms*, 1977.
- ¹²R. D. Ciskowski and C. A. Brebbia, *Boundary Element Methods in Acoustics* (Elsevier, London, 1991).
- ¹³B. Noble and J. W. Daniel, *Applied Linear Algebra* (Prentice-Hall, Englewood Cliffs, NJ, 1988).
- ¹⁴G. P. Gibbs, R. L. Clark, D. E. Cox, and J. S. Vipperman, "Radiation modal expansion: application to active structural acoustic control," *J. Acoust. Soc. Am.* **107**, 332–339 (2000).
- ¹⁵L. E. Kinsler, A. R. Frey, A. B. Coppens, and J. V. Sanders, *Fundamentals of Acoustics* (Wiley, New York, 1982).
- ¹⁶G. Hübner, "Analysis of errors in measuring machine noise under free-field conditions," *J. Acoust. Soc. Am.* **54**, 967–977 (1973).